Photoacoustics 26 (2022) 100345

Contents lists available at ScienceDirect

Photoacoustics

journal homepage: www.elsevier.com/locate/pacs

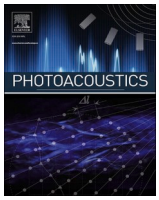

Monitoring peripheral hemodynamic response to changes in blood pressure via photoacoustic imaging

Yash Mantri [a], Tyler R. Dorobek [b], Jason Tsujimoto [a], William F. Penny [c], Pranav S. Garimella [d], Jesse V. Jokerst [b,e,f,*]

[a] Department of Bioengineering, University of California San Diego, La Jolla, CA, USA
[b] Department of Nanoengineering, University of California San Diego, La Jolla, CA, USA
[c] Department of Medicine, University of California San Diego, La Jolla, CA, USA
[d] Department of Nephrology – Hypertension, School of Medicine, University of California San Diego, La Jolla, CA, USA
[e] Materials Science Program, University of California San Diego, La Jolla, CA, USA
[f] Department of Radiology, University of California San Diego, La Jolla, CA, USA

ARTICLE INFO

Keywords:
Dialysis
Perfusion
Blood pressure
Optoacoustic imaging
Hypertension
Chronic kidney disease

ABSTRACT

Chronic wounds and amputations are common in chronic kidney disease patients needing hemodialysis (HD). HD is often complicated by drops in blood pressure (BP) called intra-dialytic hypotension. Whether intra-dialytic hypotension is associated with detectable changes in foot perfusion, a risk factor for wound formation and impaired healing remains unknown. Photoacoustic (PA) imaging is ideally suited to study perfusion changes. We scanned the feet of 20 HD and 11 healthy subjects. HD patients were scanned before and after a dialysis session whereas healthy subjects were scanned twice at rest and once after a 10 min exercise period while BP was elevated. Healthy ($r = 0.70$, $p < 0.0001$) and HD subjects ($r = 0.43$, $p < 0.01$) showed a significant correlation between PA intensity and systolic BP. Furthermore, HD cohort showed a significantly reduced PA response to changes in BP compared to the healthy controls ($p < 0.0001$), showing that PA can monitor hemodynamic changes due to changes in BP.

1. Introduction

Chronic kidney disease (CKD) affects more than 9% of the global population [1,2]. An estimated two million of these patients with CKD progress to end-stage kidney disease (ESKD) and must undergo kidney replacement therapies such as a kidney transplant or dialysis [1]. Rates of non-traumatic lower limb amputations are ~4.3/100 person-years for ESKD patients and reach 13.8/100 person-years for the diabetic sub-population [3]. Foot ulcers usually precede 84% of amputations with half occurring in diabetic patients [4]. Worse, diabetic dialysis patients develop foot ulcers at five-fold higher rate than even diabetic chronic kidney disease patients [5]. Foot ulceration is a significant risk factor for limb loss, and thus prevention—along with timely diagnosis and treatment—may translate to a reduced amputation rate. There is an urgent need to develop novel, non-invasive techniques to diagnose risk factors for ulceration and prevent limb loss in persons with ESKD.

Clinically, tissue perfusion is often inferred using measurements of blood pressure (BP) [6], blood oxygen saturation [7], and lactate levels [8]. Measurements of full body hemodynamic parameters fail to reflect changes in peripheral microcirculation [9]. Transcutaneous oxygen monitoring (TcOM) [10], functional magnetic resonance imaging (fMRI) [11], laser doppler imaging (LDI) [12], and spatial frequency domain imaging (SFDI) [13] can measure local perfusion and oxygenation in specialized care settings. TcOM is a non-invasive skin oxygen tension measurement system used for infants and adults [10]. But TcOM suffers from long acquisition times (15–20 min) and is susceptible to calibration errors and poor inter-rater usability [14]. fMRI can non-invasively image difficult to access areas like the brain and produce perfusion maps [11]. However, fMRI has poor temporal resolution (5 s) and reproducibility [15,16]. LDI can provide real-time and continuous perfusion monitoring but is sensitive to all movements resulting in erroneous readings, and it can only penetrate a few millimeters into

Abbreviations: CKD, Chronic kidney disease; ESKD, End stage kidney disease; HD, Hemodialysis; BP, Blood pressure; TcOM, Transcutaneous oxygen monitoring; fMRI, Functional magnetic resonance imaging; LDI, Laser doppler imaging.

* Correspondence to: University of California San Diego, 9500 Gilman Drive, La Jolla, CA 92093, USA.
E-mail address: jjokerst@ucsd.edu (J.V. Jokerst).

https://doi.org/10.1016/j.pacs.2022.100345
Received 15 January 2022; Received in revised form 23 February 2022; Accepted 7 March 2022
Available online 9 March 2022

tissue [17]. SFDI can provide a large field of view and rapid imaging but is limited to surface tissues and still needs to be developed further for clinical use [13].

Photoacoustic (PA) imaging is a hybrid imaging modality that can solve these major limitations. PA imaging uses pulsed light to generate sound waves via thermal expansion that can be overlaid with conventional ultrasound (US) data [18]. PA employs the difference in light absorption between oxygenated and deoxygenated hemoglobin to measure oxygen saturation, map vasculature and tissue perfusion in real time [19].

In pre-clinical settings, PA is used to measure disease biomarkers [20], oxidative stress [21,22], blood oxygen saturation [23], and image chronic wounds [24,25]. Clinically PA is used for diagnosing and monitoring breast cancer progression [26,27], vascular dynamics in human fingers [28], inflammatory bowel disease [29], and many more diseased states [30–33]. Recently, we demonstrated the ability of PA imaging to monitor angiogenesis and predict wound healing [34]. The non-invasive, real-time, and enhanced penetration depth (>4 cm) of PA imaging make it an ideal tool to map peripheral tissue perfusion as a risk factor for the development of limb complications.

Here, we aimed to explore the use of PA to measure changes in peripheral blood perfusion in a cohort of HD patients before and after dialysis. We hypothesized that the change in PA signal would be dependent on changes in blood pressure given the intradialytic hypotension that often occurs in patients [35–39]. The loss of pressure is followed by peripheral vasoconstriction and reduced peripheral perfusion because blood flow is redirected towards the vital organs [40]. This controlled change in blood pressure in a resting patient without medication or exercise is unique to HD patients. Hence HD patients make an exquisite cohort to study the effects of blood pressure on peripheral photoacoustic signals and tissue perfusion.

2. Methods

2.1. Participants

This study was performed in accordance with the ethical guidelines for human experimentation stated in the 1975 Declaration of Helsinki. The study was approved by the University of California San Diego's Human Research Protections Program and was given Institutional Review Board approval (IRB# 191998). Written informed consent was obtained from all subjects before participation. All subjects were ≥ 18 years old and able to provide consent. Exclusion criteria were: (i) presence of bloodborne pathogens and (ii) presence of implants in the imaging region. Dialysis patients (n = 22) were recruited consecutively for this study at the outpatient hemodialysis Unit at UC San Diego Health System. Eleven healthy volunteers, with no known vascular disease history were recruited at UC San Diego.

The dialysis patients were each scanned twice: once at the start of HD (pre-dialysis), and again at the completion of HD (post-dialysis). Blood pressure and ultrafiltration volume were recorded by the Fresenius 2008 T dialyzer (Fresenius Medical Care, Waltham, MA, USA). Two of the 22 dialysis patients were subsequently excluded from the analysis due to complications during HD (unrelated to imaging) preventing a post HD scan.

The 11 healthy subjects were each scanned three times: 1) at baseline; 2) after 3 h of rest and no pressure changes (negative control (test/re-test), pre-exercise); and 3) after 10 min of exercise to elevate blood pressure (positive control, post-exercise). We monitored body temperature, heart rate (HR), and blood pressure (BP) at all imaging time points. Fig. 1 illustrates the study protocol for the two groups. Table 1 describes the HD and healthy group demographics.

2.2. Blood pressure measurements

Blood pressure (BP) for the HD patients was measured automatically by the dialyzer (Fresenius 2008T, Fresenius North America, Waltham, MA). We also noted their ultrafiltration volume at the end of the HD session. Patients were at rest sitting in semi-Fowler's position at the time of measurement. BP measurements were made just before and at completion of the HD session (Fig. 1D). Change in systolic pressure was defined as the difference between BP_{HDend} and $BP_{HDstart}$.

For the healthy group we used an electronic blood pressure monitor (Omcron Healthcare Inc., Lake Forest, IL, USA, Model no: BP742N). The cuff was placed on the left upper arm and the subjects were sitting up straight for all measurements. We recorded BP twice at rest (T = 0 and T = 3 h) and once after 10 min of exercise (Fig. 1C). The T = 3 hrs time point was chosen to mimic the length of a typical HD session without changes in BP, serving as a negative control. Exercise consisted of

Table 1
HD and Healthy group demographics.

Category	HD group (n = 22)	Healthy group (n = 11)
Age (mean ± SD)	59.2 ± 14.3 years	26.5 ± 4.1 years
Male/Female	7/15	11/0
Diabetic/non-diabetic	14/8	0/11
Average UF removed	2732.3 ± 1109 ml	N.A.

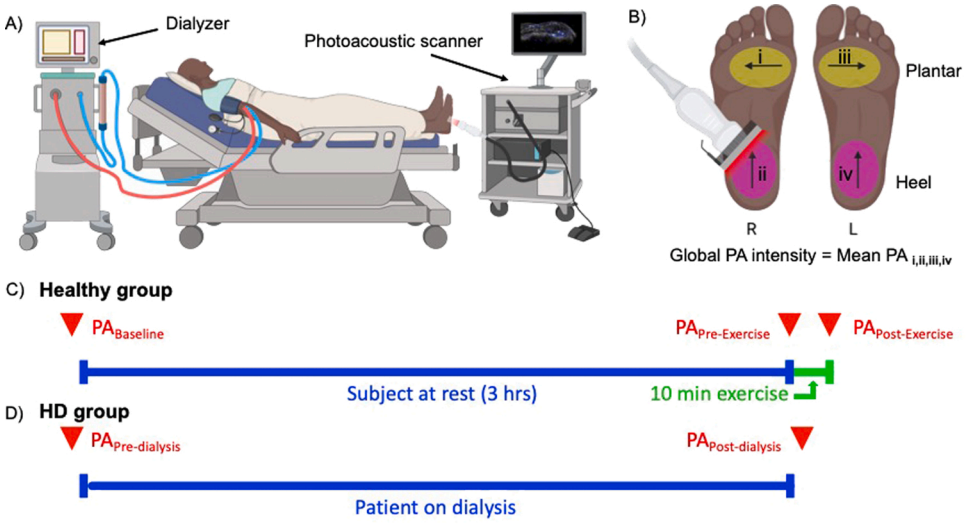

Fig. 1. Photoacoustic monitoring of peripheral perfusion; study design and timeline. A. The HD group consisted of patients on hemodialysis (HD). B. We scanned the plantar and heel area in a medial-lateral and inferior-superior direction, respectively. Global PA intensity was defined as the mean PA intensity of all four imaging regions. C. Healthy subjects were scanned at baseline (T = 0 hrs), pre-exercise (T = 3 hrs), and immediately after 10 min of exercise (post-exercise). D. HD patients were scanned pre-and-post their HD session. Red downward triangles represent imaging time points. Blue line indicated healthy subjects at rest for 3 hrs and HD patients on dialysis. Green denotes the 10 min exercise period to increase blood pressure in healthy subjects.

climbing up and down stairs for 10 min to simulate an increase in blood pressure (positive control). Changes in systolic BP were calculated as differences between (i) $BP_{pre\text{-}exercise}$ and $BP_{baseline}$; and (ii) $BP_{post\text{-}exercise}$ - $BP_{pre\text{-}exercise}$.

2.3. Photoacoustic imaging

All the PA imaging was done using the AcousticX from Cyberdyne Inc. (Tsukuba, Japan). This LED-based PA scanner operates at 850 nm wavelength with an LED repetition rate of 4 kHz, pulse width of 70 ns, and operating at 2.6 μJ/cm^2 per pulse [41]. It employs a 128-element linear array transducer with a 0.38 × 6 cm field of view, 7 MHz central frequency, and a bandwidth of 80.9% [42]. We used a custom hydrophobic gel pad from Cyberdyne Inc. along with sterile US coupling gel (Aquasonic 100, Parker Laboratories Inc. Fairfield NJ, USA) to couple the transducer with the skin surface. A sterile sleeve (CIV-Flex™ #921191 from AliMed Inc., Dedham, MA, USA) covered the transducer during imaging. All images were acquired at 30 frames/s in a single handheld sweep.

We scanned two spots on each foot (except for one patient in whom only one foot was scanned due to a left lower limb amputation). The plantar area was scanned in a medial-lateral direction and the heel area in an inferior-superior direction (Fig. 1B). It must be noted that since all the scans are done manually, precise control of the scan area was extremely difficult. But the same general area was scanned for every patient. HD patients were scanned once before and once after an HD session (Fig. 1D). Healthy subjects (the control group) were scanned three times (Fig. 1C). BP measurements and PA imaging were carried out simultaneously.

2.4. Image processing

All scans were reconstructed and visualized using the proprietary AcousticX software (Cyberdyne Inc. version 2.00.10); 8-bit PA, B-mode, and PA+US overlayed coronal cross-sectional images were exported. We used the proprietary software developed by the PA system's manufacturer for image reconstruction. The system reconstructs PA images using Fourier transform analysis [41]. All the processing was done manually. Scans ranged between 45 and 180 frames governed by scan distance and length. PA signal was quantified using region of interest (ROI) analysis via ImageJ (with Fiji extension), version 2.1.0/1.53c. We drew a 4-cm-wide and 1-cm-deep rectangular ROI that was kept constant across all frames. PA signal from the skin was excluded from analysis to minimize the impact of variable melanin concentration in different skin tones. Integrated density function was used to quantify the PA signal within the ROI. Global PA intensity was defined as the mean integrated PA density of all four imaging regions (Fig. 1B).

2.5. Statistics

We measured changes in PA intensity as a function of changes in systolic BP. Simple linear regression was used to fit this data and plotted with 95% confidence intervals. We used a paired, two-tailed t-test to compare PA intensities pre-and-post exercise and HD for the healthy and diseased groups, respectively. We also used a student's t-test to compare the hemodynamic response to changes in blood pressure for HD vs. healthy subjects. A p-value < 0.05 was considered significant. We tested equality of the two population variances (Healthy vs. HD group) using a one-tailed F-test with an alpha $= 0.05$. The difference was considered significant if the F-value was less than the $F_{critical}$ value. We also ran two separate multivariate linear regressions (HD and healthy group) to study the effect of other confounding variables such as body mass index (BMI in kg/m^2), diabetic status (Y/N), UF removed (ml), age (years), sex (M/F). A covariance matrix was also calculated to study the effect of the confounding variables on each other. Future work will evaluate heart rate and body temperature in this multivariate analysis.

3. Results

A total of 33 subjects were recruited for this study. All subjects were pseudonymized with an identification code at the start of the study. The healthy and the HD group are referred as HC 0XX and CKD/HD 0YY respectively. Patient demographics and BP data can be found in Tables S1 (Healthy) and S2 (HD).

3.1. Healthy control group

Eleven subjects (26.5 ± 4.1 years old) with no history of cardiovascular or other disease were recruited at UCSD. Subjects were scanned at baseline (T = 0 hrs), pre-exercise at rest (T = 3 h), and immediately post-exercise (Fig. 2A). Exercising consisted of climbing up and down stairs for 10 min. We monitored BP, heart rate, and body temperature at each imaging time point (Table S1). Fig. 2 shows PA data from the healthy cohort.

The PA signal under the skin surface increased by 47% ($p < 0.01$), and the average BP increased by 27.6 ± 18.2 mmHg immediately post-exercise relative to baseline (Fig. 2 B-C). The change in PA intensity was directly ($r = 0.81$) and significantly ($p < 0.0001$) proportional to the change in systolic BP (Fig. 2D). PA intensity was significantly ($p < 0.0001$) higher after exercise when BP was elevated (Fig. 2C). As a negative control, the subjects were maintained at rest for 3 hrs, simulating the length of a typical HD session. There were no significant changes in BP and PA intensity (baseline - pre-exercise) during the rest period ($p = 0.18$).

3.2. HD group

Twenty-two HD patients were enrolled in this cohort (59.2 ± 14.3 years old). Two patients developed hypotension-related complications preventing a second scan and were not included the analysis due to incomplete data acquisition (Table S2). The complications were independent of the imaging study. Patients were scanned before and after a routine HD session (Fig. 3B).

On average PA signal and systolic BP reduced by 11% and 16.6 ± 19.8 mm of Hg respectively. PA intensity and hence perfusion was significantly lower after dialysis (Fig. 3C, $p < 0.01$). PA intensity in different imaging regions trended lower after dialysis but the difference was not statistically significant. PA intensity showed a positive correlation to changes in BP during an HD session ($r = 0.43$, $p < 0.01$, Fig. 3E). PA signal and hence perfusion was higher pre-dialysis when BP was higher. The UF removed showed a positive correlation with BP but did not directly correlate with the change in PA intensity (Fig. S4).

3.3. Healthy vs. HD subjects

HD patients showed a significantly different PA response to changes in BP compared to healthy controls (Fig. 4). The mean PA intensity was significantly higher for the HD group (Fig. 4A, $p < 0.01$). More importantly, the data spread (standard deviation) for the diseased group was significantly wider ($F = 0.045$; $F_{critical} = 0.63$). The hemodynamic response to changes in BP was characterized using the slope of changing PA as a function of changing systolic pressure (Fig. 4B). The slope for the HD group (1870 a.u. intensity/mm Hg) was significantly ($p = 0.0001$) lower than the healthy group (5116 a.u. intensity/mm Hg).

4. Discussion

This cohort study explored the use of photoacoustic imaging to compare changes in peripheral perfusion in response to varying BP in HD patients vs. healthy controls. Our data suggests that HD patients show a significantly reduced PA response ($p = 0.0001$) to changes in BP compared to healthy controls.

The removal of excess fluid via ultrafiltration increases hematocrit

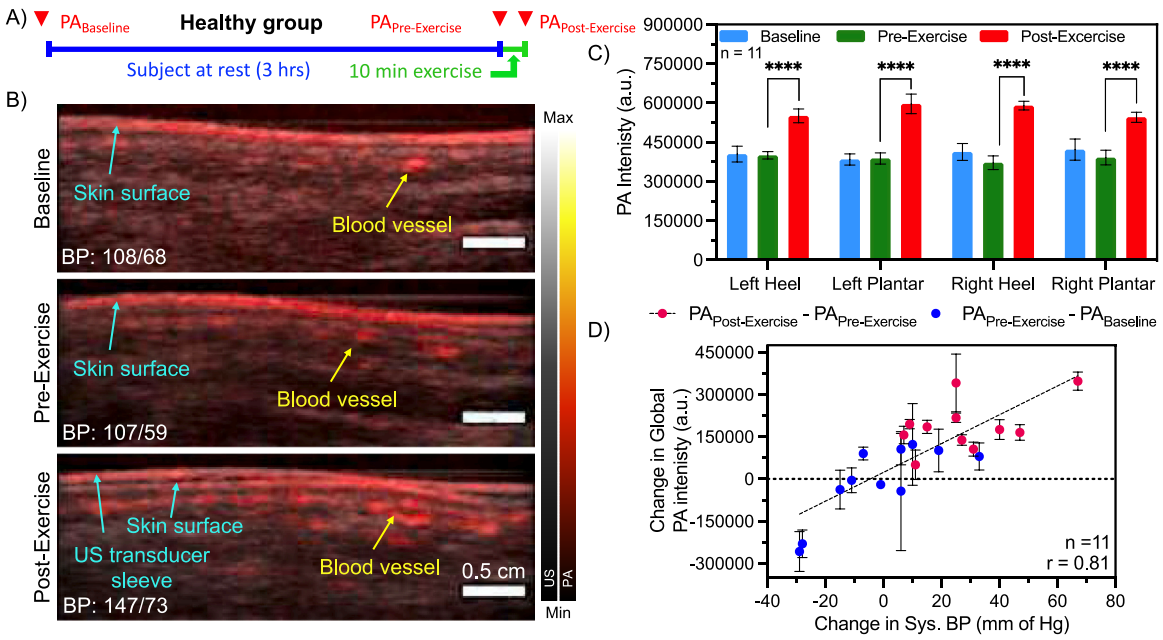

Fig. 2. Hemodynamic response to changes in blood pressure for healthy subjects. A. Study design for the healthy group. Subjects were scanned at baseline (T = 0 hrs), pre-exercise at rest (T = 3 hrs), and immediately post-exercise. B. PA and US overlay of the left heel (HC 002). Blood vessels appear as distinct red dots marked by the yellow arrow. The skin surface is labelled in blue. At rest there was negligible change in systolic BP between baseline and pre-exercise. After a 10 min exercise session, blood pressure increased by 40 mm of Hg accompanied by a higher PA signal. PA intensity was quantified using a rectangular ROI measuring 4 cm × 1 cm. The skin surface was excluded from analysis. The ROI annotated images can be found in the Supplementary information. Scale bar represents 0.5 cm. C. PA intensity was significantly higher after exercise (****, $p < 0.0001$, n = 11) at each imaging site. There were no significant differences between $PA_{Baseline}$ and $PA_{Pre\text{-}Exercise}$. This rest period served as a negative control for the healthy group. D. The change in global PA intensity in the healthy group correlated with the change in systolic BP ($r = 0.81$, $p < 0.001$). The 22 data points reflect changes between $PA_{Pre\text{-}Exercise} - PA_{Baseline}$ (Blue) and $PA_{Post\text{-}Exercise} - PA_{Pre\text{-}Exercise}$ (Pink) (n = 11). Error bars in panel C represent standard deviation between 11 subjects and in panel D at least 90 frames.

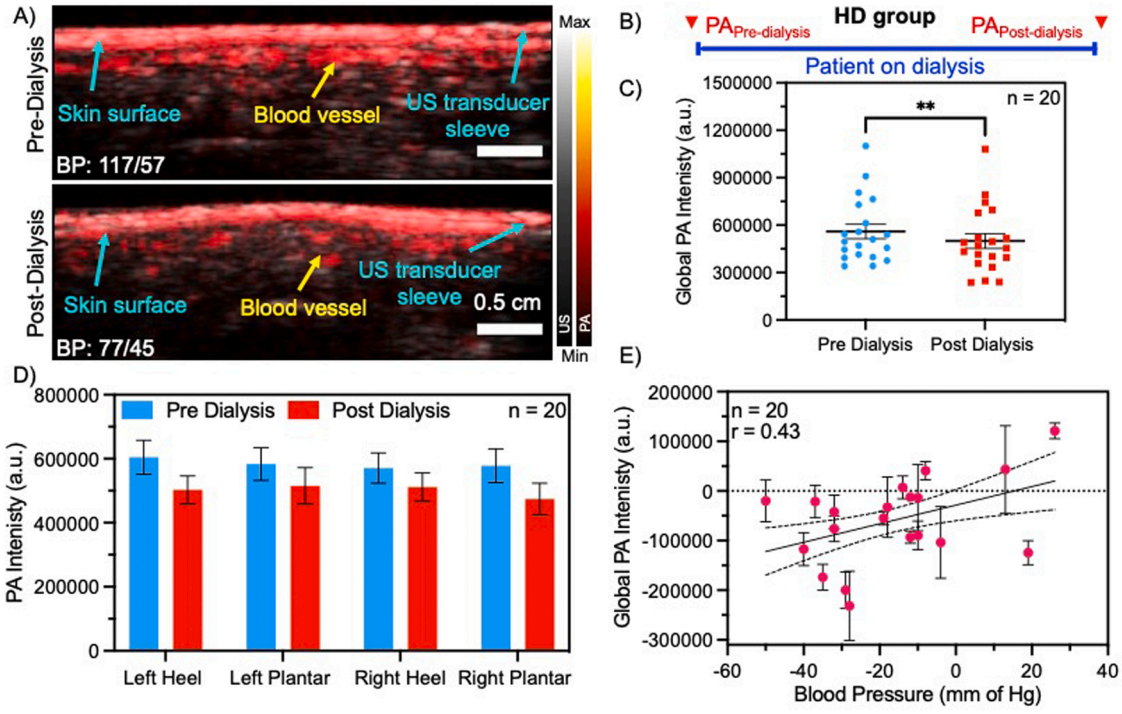

Fig. 3. Changes in peripheral tissue perfusion during hemodialysis. A. PA and US overlay of the left heel in subject HD 012. Blood perfusion into the heel is considerably lower after dialysis when BP is low. Scale bar represents 0.5 cm. B. HD patients were scanned just before and after a routine dialysis session. C. A paired t-test showed a significant decrease in global PA signal and hence perfusion after dialysis (**, $p < 0.01$). D. PA intensity at individual imaging areas were lower (not significantly) after dialysis. E. Hemodynamic response of the HD group to changes in BP during dialysis showed a positive correlation ($r = 0.43$, $p < 0.01$). Error bars in panel C-D represent standard deviation among 20 patients and in panel E at least 90 frames.

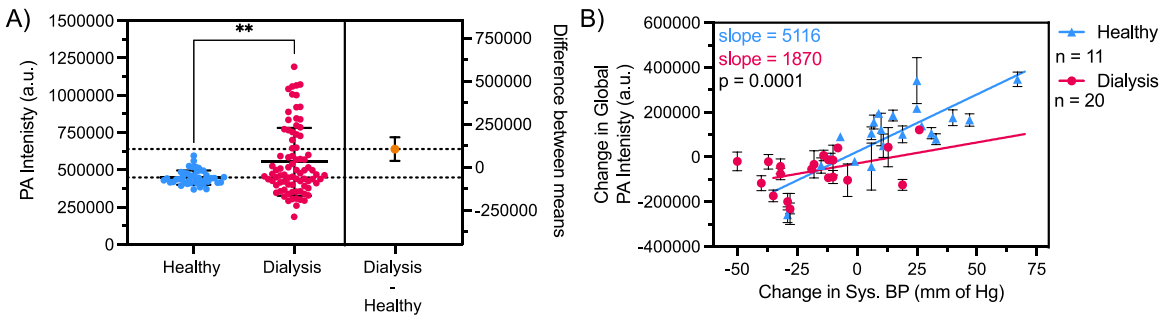

Fig. 4. Comparing hemodynamic response to changes in BP in health vs. dialysis patients. A. PA intensities of the healthy and diseased group for all scans. HD show a significantly wider PA distribution ($F = 0.045$; $F_{critical} = 0.63$) compared to the healthy group. Dialysis patients also showed a significantly higher (**, $p < 0.01$) mean PA intensity compared to healthy control group due to higher mean BP. B. Healthy subjects showed a significantly higher slope (significant difference between slopes; $p = 0.0001$) to changes in BP compared to the HD patients. The slope of the simple linear regression characterizes the hemodynamic response to changes in BP. Error bars in panel A represent standard deviation among all scans ($n_{healthy} = 44$; $n_{diseased} = 80$) and in panel B at least 90 frames.

[35]. Since PA leverages hemoglobin in red blood cells to generate contrast, the increase in hematocrit should increase PA intensity after dialysis [43,44]. But we observed the opposite effect: The global PA intensity significantly decreases after HD (Fig. 3C, $p < 0.01$). This can be attributed to the reduction of BP after dialysis. A sudden drop in blood pressure results in peripheral vasoconstriction as blood is shunted towards the vital organs to preserve their function [45]. Vasoconstriction results in reduced peripheral perfusion that is observed as lower PA intensity after HD. Hypertension is present in 68% of HD patients, and this further reduces peripheral perfusion [46]. The changes in peripheral perfusion can exacerbate the risk of developing complications such as ulceration, amputations, and cardiovascular morbidity [47–49].

The management of intradialytic hypotension in HD patients is challenging and extremely important. A sudden drop in BP can leave patients lethargic and weak [50]. Some patients show a paradoxical rise in blood pressure after dialysis due to an increased cardiac output and hematocrit [51,52]. Three HD patients (13.6%) showed a paradoxical rise in BP in the HD cohort, which might explain why individual imaging regions showed no significant difference before and after dialysis (Fig. 3D). Instead, a paired comparison of the global PA intensity in Fig. 3C showed a statistically significant difference ($p < 0.01$).

The main clinical finding of this work is that photoacoustic imaging can be used to differentiate between a healthy and diseased response to changes in BP (Fig. 4B). The slopes characterize the change in perfusion as a function of BP. The healthy control cohort showed a significantly higher perfusion ($p = 0.0001$) when BP was elevated compared to the HD cohort. HD patients had a significantly wider distribution of PA intensities due to higher variability in BP compared to the control group (HD: 135.4 ± 29.1 mm of Hg; Healthy: 137.3 ± 19.4 mm of Hg, Fig. 4A). Although this cohort study was not age and gender matched, we have 85% power in our results (Fig. S5). Furthermore, the healthy group showed a significant positive correlation between global PA intensity and absolute systolic BP (Fig. S6, $r = 0.70$, $p < 0.05$) at baseline. The HD group showed no significant correlation which can be attributed to varying disease etiologies and progression. Hence, this work suggests that PA imaging can be used to monitor peripheral tissue perfusion, a risk factor for wound formation and impaired healing [53,54]. Others have also shown the use of PA imaging to visualize tissue perfusion but most studies use high-powered lasers which are expensive, bulky, and pose an exposure risk above the maximum permissible exposure limit [28,55,56].

Whether these changes in perfusion pose a significant risk to HD patients remains to be seen. A future longitudinal study predicting wound formation and correlating changes in perfusion with wound healing will help clinicians tailor therapeutic regimes to best serve each patient. For example, patients with poor perfusion can be provided advanced therapies such as hyperbaric oxygen therapy (HBOT) that are known to promote angiogenesis, perfusion, and wound healing [57].

Changes in BP are also dependent on other confounding factors such as BMI [58], diabetic status [59], age [60] etc. A multivariate linear regression (Fig. S7) shows a strong positive correlation ($R = 0.72$) accounting for seven such confounding variables. Furthermore, the covariance matrix shows that the volume of UF removed has strong and positive covariance with the change in systolic pressure. Patients who had high volumes of UF removed, tended to show higher changes in pressure. In the healthy group (Fig. S8), the main contributing variable was the change in systolic BP ($R = 0.81$) whereas all the other confounding variables had relatively low covariance with each other. This means that the contributor to PA change was the change in systolic BP ($p = 0.0019$). Melanin, the molecule that gives skin its characteristic color is also a major absorber and source of PA signal [61]. Our group recently studied the effect of skin tone on PA oximetry [61]. In this work, we excluded any signals from the skin surface and since patients serve as their own controls between scans, and we only evaluated the change between scans; thus, skin tone should have minimal impacts. Furthermore, this study recruited a diverse set of HD patients and HD subjects from all possible skin types (Fitzpatrick scores 1–6) to account for skin tone bias. Other confounding variables could be changes in vascular physiology (increased resistance, calcification etc.) due to chronic diseased states in the HD groups [62], but these are extremely difficult to account for.

4.1. Limitations

The LED-based PA system used in this work is an inexpensive, portable, and non-invasive imaging system. The LEDs used in this system operate 1000-fold under the maximum permissible exposure limit of 20 mJ/cm^2 [63]. But the system is limited in data processing as it condenses the number of frames between acquisition and export. Since we used a handheld scanner for all scans, it is difficult to generate 3D maps of the imaging area even though the system is capable to do so. The use of motion compensation and deep-learning algorithms to reduce noise and align frames could help map perfusion and oxygenation of the tissue [64,65]. Future work will look to map tissue oxygenation in real time.

Within the HD group, hematocrit readings could help normalize PA intensity changes for variable fluid loss between patients. But not all dialyzers were equipped to measure hematocrit in real time limiting our analysis.

5. Conclusion

The management of BP and peripheral perfusion in dialysis patients is extremely important and challenging to monitor. Peripheral perfusion measurements are rare at the point-of-care. In this work, we imaged peripheral perfusion in 20 HD patients and 11 healthy subjects using PA imaging. We compared the peripheral tissue perfusion response to

changes in blood pressure due to dialysis or exercise. The healthy group showed a positive correlation to changes in BP. The HD group also showed a positive correlation to BP changes during a dialysis session. In comparison, the HD group showed a significantly reduced PA response to changes in blood pressure compared to healthy controls.

Declaration of Competing Interest

The authors declare that they have no known competing financial interests or personal relationships that could have appeared to influence the work reported in this paper.

Data Availability

The raw anonymized data that supports the findings of this study are available on reasonable request from the corresponding author.

Acknowledgments

Fig. 1A-B were created with BioRender.com. This work was supported by the National Institutes of Health through R21 AG065776 as well as internal funds from UCSD under the Galvanizing Engineering in Medicine program. PG acknowledges funding from the National Institute of Diabetes and Digestive and Kidney Diseases through K23 DK114556. YM and TD would like to acknowledge help from Yvette Waters, RN, BSN, CNN and the entire nursing team at the outpatient hemodialysis unit, UC San Diego Medical Center, Hillcrest, San Diego, CA, USA.

Appendix A. Supporting information

Supplementary data associated with this article can be found in the online version at doi:10.1016/j.pacs.2022.100345.

References

[1] A.C. Webster, E.V. Nagler, R.L. Morton, P. Masson, Chronic kidney disease, lancet 389 (10075) (2017) 1238–1252.
[2] B. Bikbov, C.A. Purcell, A.S. Levey, M. Smith, A. Abdoli, M. Abebe, O.M. Adebayo, M. Afarideh, S.K. Agarwal, M. Agudelo-Botero, Global, regional, and national burden of chronic kidney disease, 1990–2017: a systematic analysis for the Global Burden of Disease Study 2017, Lancet 395 (10225) (2020) 709–733.
[3] P.W. Eggers, D. Gohdes, J. Pugh, Nontraumatic lower extremity amputations in the Medicare end-stage renal disease population, Kidney Int. 56 (4) (1999) 1524–1533.
[4] R.E. Pecoraro, G.E. Reiber, E.M. Burgess, Pathways to diabetic limb amputation. Basis for prevention, Diabetes Care 13 (5) (1990) 513–521.
[5] A. Ndip, M.K. Rutter, L. Vileikyte, A. Vardhan, A. Asari, M. Jameel, H.A. Tahir, L. A. Lavery, A.J. Boulton, Dialysis treatment is an independent risk factor for foot ulceration in patients with diabetes and stage 4 or 5 chronic kidney disease, Diabetes Care 33 (8) (2010) 1811–1816.
[6] S. Magder, The meaning of blood pressure, Crit. Care 22 (1) (2018) 1–10.
[7] J.-L. Vincent, J.-J. Moraine, P. Van Der Linden, Toe temperature versus transcutaneous oxygen tension monitoring during acute circulatory failure, Intensive Care Med. 14 (1) (1988) 64–68.
[8] F.G. Zampieri, L.P. Damiani, J. Bakker, G.A. Ospina-Tascón, R. Castro, A. B. Cavalcanti, G. Hernandez, Effects of a resuscitation strategy targeting peripheral perfusion status versus serum lactate levels among patients with septic shock. A Bayesian Reanalysis of the ANDROMEDA-SHOCK Trial, Am. J. Respir. Crit. care Med. 201 (4) (2020) 423–429.
[9] A. Lima, J. Bakker, Noninvasive monitoring of peripheral perfusion, Appl. Physiol. Intensive Care Med. (2006) 131–141.
[10] M.M. Kmiec, H. Hou, M. Lakshmi Kuppusamy, T.M. Drews, A.M. Prabhat, S. V. Petryakov, E. Demidenko, P.E. Schaner, J.C. Buckey, A. Blank, Transcutaneous oxygen measurement in humans using a paramagnetic skin adhesive film, Magn. Reson. Med. 81 (2) (2019) 781–794.
[11] G.K. Aguirre, J.A. Detre, J. Wang, Perfusion fMRI for functional neuroimaging, Int. Rev. Neurobiol. 66 (2005) 213–236.
[12] M. Leahy, F. De Mul, G. Nilsson, R. Maniewski, Principles and practice of the laser-Doppler perfusion technique, Technol. Health Care 7 (2–3) (1999) 143–162.
[13] S. Gioux, A. Mazhar, D.J. Cuccia, Spatial frequency domain imaging in 2019: principles, applications, and perspectives, J. Biomed. Opt. 24 (7) (2019), 071613.
[14] A. Ercengiz, M. Mutluoglu, Hyperbaric Transcutaneous Oximetry, 2017.
[15] K. Specht, Current challenges in translational and clinical fMRI and future directions, Front. Psychiatry 10 (2020) 924.
[16] C.M. Bennett, M.B. Miller, G.L. Wolford, Neural correlates of interspecies perspective taking in the post-mortem Atlantic Salmon: An argument for multiple comparisons correction, Neuroimage 47 (Suppl 1) (2009). S125.
[17] B. Fagrell, G. Nilsson, Advantages and limitations of one-point laser Doppler perfusion monitoring in clinical practice, Vasc. Med. Rev. 2 (1995) 97–101.
[18] Y. Mantri, J.V. Jokerst, Engineering plasmonic nanoparticles for enhanced photoacoustic imaging, ACS Nano 14 (8) (2020) 9408–9422.
[19] M. Xu, L.V. Wang, Photoacoustic imaging in biomedicine, Rev. Sci. Instrum. 77 (4) (2006), 041101.
[20] C. Moore, R.M. Borum, Y. Mantri, M. Xu, P. Fajtová, A.J. O'Donoghue, J.V. Jokerst, Activatable carbocyanine dimers for photoacoustic and fluorescent detection of protease activity, ACS Sens. (2021).
[21] Y. Mantri, B. Davidi, J.E. Lemaster, A. Hariri, J.V. Jokerst, Iodide-doped precious metal nanoparticles: measuring oxidative stress in vivo via photoacoustic imaging, Nanoscale 12 (19) (2020) 10511–10520.
[22] A. Hariri, E. Zhao, A.S. Jeevarathinam, J. Lemaster, J. Zhang, J.V. Jokerst, Molecular imaging of oxidative stress using an LED-based photoacoustic imaging system, Sci. Rep. 9 (1) (2019) 1–10.
[23] A. Hariri, J. Wang, Y. Kim, A. Jhunjhunwala, D.L. Chao, J.V. Jokerst, In vivo photoacoustic imaging of chorioretinal oxygen gradients, J. Biomed. Opt. 23 (3) (2018), 036005.
[24] A. Hariri, F. Chen, C. Moore, J.V. Jokerst, Noninvasive staging of pressure ulcers using photoacoustic imaging, Wound Repair Regen. 27 (5) (2019) 488–496.
[25] Y. Wang, Y. Zhan, L.M. Harris, S. Khan, J. Xia, A portable three-dimensional photoacoustic tomography system for imaging of chronic foot ulcers, Quant. Imaging Med. Surg. 9 (5) (2019) 799.
[26] N. Nyayapathi, J. Xia, Photoacoustic imaging of breast cancer: a mini review of system design and image features, J. Biomed. Opt. 24 (12) (2019), 121911.
[27] N. Nyayapathi, H. Zhang, E. Zheng, S. Nagarajan, E. Bonaccio, K. Takabe, X.C. Fan, J. Xia, Photoacoustic dual-scan mammoscope: results from 38 patients, Biomed. Opt. Express 12 (4) (2021) 2054–2063.
[28] J. Ahn, J.Y. Kim, W. Choi, C. Kim, High-resolution functional photoacoustic monitoring of vascular dynamics in human fingers, Photoacoustics 23 (2021), 100282.
[29] M.J. Waldner, F. Knieling, C. Egger, S. Morscher, J. Claussen, M. Vetter, C. Kielisch, S. Fischer, L. Pfeifer, A. Hagel, Multispectral optoacoustic tomography in Crohn's disease: noninvasive imaging of disease activity, Gastroenterology 151 (2) (2016) 238–240.
[30] A.P. Regensburger, A.L. Wagner, J. Claussen, M.J. Waldner, F. Knieling, Shedding light on pediatric diseases: multispectral optoacoustic tomography at the doorway to clinical applications, Mol. Cell. Pediatr. 7 (1) (2020) 1–6.
[31] A.P. Regensburger, A.L. Wagner, V. Danko, J. Jüngert, A. Federle, D. Klett, S. Schuessler, A. Buehler, M.F. Neurath, A. Roos, Multispectral optoacoustic tomography for non-invasive disease phenotyping in pediatric spinal muscular atrophy patients, Photoacoustics 25 (2022), 100315.
[32] S. Manohar, S. Gambhir, Clinical photoacoustic imaging, Photoacoustics 19 (2020).
[33] A.B.E. Attia, G. Balasundaram, M. Moothanchery, U. Dinish, R. Bi, V. Ntziachristos, M. Olivo, A review of clinical photoacoustic imaging: current and future trends, Photoacoustics 16 (2019), 100144.
[34] Y. Mantri, J. Tsujimoto, B. Donovan, C.C. Fernandes, P.S. Garimella, W.F. Penny, C. A. Anderson, J.V. Jokerst, Photoacoustic monitoring of angiogenesis predicts response to therapy in healing wounds, Wound Repair and Regeneration (2021).
[35] J. Himmelfarb, T.A. Ikizler, Hemodialysis, New Engl. J. Med. 363 (19) (2010) 1833–1845.
[36] B. Charra, Fluid balance, dry weight, and blood pressure in dialysis, Hemodial. Int. 11 (1) (2007) 21–31.
[37] Q. Maggiore, F. Pizzarelli, A. Santoro, G. Panzetta, G. Bonforte, T. Hannedouche, M.A.A. de Lara, I. Tsouras, A. Loureiro, P. Ponce, The effects of control of thermal balance on vascular stability in hemodialysis patients: results of the European randomized clinical trial, Am. J. Kidney Dis. 40 (2) (2002) 280–290.
[38] B.V. Stefánsson, S.M. Brunelli, C. Cabrera, D. Rosenbaum, E. Anum, K. Ramakrishnan, D.E. Jensen, N.-O. Stålhammar, Intradialytic hypotension and risk of cardiovascular disease, Clin. J. Am. Soc. Nephrol. 9 (12) (2014) 2124–2132.
[39] Q. Maggiore, Isothermic dialysis for hypotension-prone patients, Semin. Dial. (2002) 187–190. Wiley Online Library.
[40] T.W. Secomb, Hemodynamics, Compr. Physiol. 6 (2) (2016) 975.
[41] A. Hariri, J. Lemaster, J. Wang, A.S. Jeevarathinam, D.L. Chao, J.V. Jokerst, The characterization of an economic and portable LED-based photoacoustic imaging system to facilitate molecular imaging, Photoacoustics 9 (2018) 10–20.
[42] E. Maneas, R. Aughwane, N. Huynh, W. Xia, R. Ansari, M. Kuniyil Ajith Singh, J. C. Hutchinson, N.J. Sebire, O.J. Arthurs, J. Deprest, Photoacoustic imaging of the human placental vasculature, J. Biophotonics 13 (4) (2020) e201900167.
[43] R.K. Saha, M.C. Kolios, A simulation study on photoacoustic signals from red blood cells, J. Acoust. Soc. Am. 129 (5) (2011) 2935–2943.
[44] E. Hysi, R.K. Saha, M.C. Kolios, On the use of photoacoustics to detect red blood cell aggregation, Biomed. Opt. Express 3 (9) (2012) 2326–2338.
[45] E. Ozakin, N.O. Yazlamaz, F.B. Kaya, E.M. Karakilic, M. Bilgin, Perfusion index measurement in predicting hypovolemic shock in trauma patients, J. Emerg. Med. 59 (2) (2020) 238–245.
[46] D. Bolignano, S. Rastelli, R. Agarwal, D. Fliser, Z. Massy, A. Ortiz, A. Wiecek, A. Martinez-Castelao, A. Covic, D. Goldsmith, Pulmonary hypertension in CKD, Am. J. Kidney Dis. 61 (4) (2013) 612–622.
[47] J.E. Flythe, S.E. Kimmel, S.M. Brunelli, Rapid fluid removal during dialysis is associated with cardiovascular morbidity and mortality, Kidney Int. 79 (2) (2011) 250–257.

[48] L.A. Lavery, D.C. Lavery, N.A. Hunt, J. La Fontaine, A. Ndip, A.J. Boulton, Amputations and foot-related hospitalisations disproportionately affect dialysis patients, Int. Wound J. 12 (5) (2015) 523–526.
[49] M. Meloni, V. Izzo, L. Giurato, V. Cervelli, R. Gandini, L. Uccioli, Impact of heart failure and dialysis in the prognosis of diabetic patients with ischemic foot ulcers, J. Clin. Transl. Endocrinol. 11 (2018) 31–35.
[50] N. Evangelidis, B. Sautenet, K.E. Manera, M. Howell, J.C. Craig, A.K. Viecelli, E. O'Lone, N. Scholes-Robertson, D.W. Johnson, Y. Cho, Perspectives on blood pressure by patients on haemo-and peritoneal dialysis, Nephrology 26 (1) (2021) 62–69.
[51] A.I. Günal, I. Karaca, H. Celiker, E. Ilkay, S. Duman, Paradoxical rise in blood pressure during ultrafiltration is caused by increased cardiac output, J. Nephrol. 15 (1) (2002) 42–47.
[52] M. Cirillo, M. Laurenzi, M. Trevisan, J. Stamler, Hematocrit, blood pressure, and hypertension. The gubbio population study, Hypertension 20 (3) (1992) 319–326.
[53] Y. Mantri, J. Tsujimoto, B. Donovan, C.C. Fernandes, P.S. Garimella, W.F. Penny, C. A. Anderson, J.V. Jokerst, Photoacoustic monitoring of angiogenesis predicts response to therapy in healing wounds, medRxiv, 2021.
[54] M. Makhsous, M. Priebe, J. Bankard, R. Rowles, M. Zeigler, D. Chen, F. Lin, Measuring tissue perfusion during pressure relief maneuvers: insights into preventing pressure ulcers, J. Spinal Cord. Med. 30 (5) (2007) 497–507.
[55] M. Choi, A.J. Shapiro, R. Zemp, Tissue perfusion rate estimation with compression-based photoacoustic-ultrasound imaging, J. Biomed. Opt. 23 (1) (2018), 016010.
[56] E. Zhang, J. Laufer, R. Pedley, P. Beard, In vivo high-resolution 3D photoacoustic imaging of superficial vascular anatomy, Phys. Med. Biol. 54 (4) (2009) 1035.
[57] R.J. Goldman, Hyperbaric oxygen therapy for wound healing and limb salvage: a systematic review, PM&R 1 (5) (2009) 471–489.
[58] Z. Gundogdu, Relationship between BMI and blood pressure in girls and boys, Public Health Nutr. 11 (10) (2008) 1085–1088.
[59] G.L. Bakris, The importance of blood pressure control in the patient with diabetes, Am. J. Med. 116 (5) (2004) 30–38.
[60] S. Landahl, C. Bengtsson, J.A. Sigurdsson, A. Svanborg, K. Svärdsudd, Age-related changes in blood pressure, Hypertension 8 (11) (1986) 1044–1049.
[61] Y. Mantri, J.V. Jokerst, Impact of skin tone on photoacoustic oximetry and tools to minimize bias, Biomed. Opt. Express 13 (2) (2022) 875–887.
[62] R.C. Shroff, R. McNair, N. Figg, J.N. Skepper, L. Schurgers, A. Gupta, M. Hiorns, A. E. Donald, J. Deanfield, L. Rees, Dialysis accelerates medial vascular calcification in part by triggering smooth muscle cell apoptosis, Circulation 118 (17) (2008) 1748–1757.
[63] R. Manwar, X. Li, S. Mahmoodkalayeh, E. Asano, D. Zhu, K. Avanaki, Deep learning protocol for improved photoacoustic brain imaging, J. Biophotonics 13 (10) (2020), e202000212.
[64] A. Hariri, K. Alipour, Y. Mantri, J.P. Schulze, J.V. Jokerst, Deep learning improves contrast in low-fluence photoacoustic imaging, Biomed. Opt. Express 11 (6) (2020) 3360–3373.
[65] M. Mozaffarzadeh, C. Moore, E.B. Golmoghani, Y. Mantri, A. Hariri, A. Jorns, L. Fu, M.D. Verweij, M. Orooji, N. de Jong, Motion-compensated noninvasive periodontal health monitoring using handheld and motor-based photoacoustic-ultrasound imaging systems, Biomed. Opt. Express 12 (3) (2021) 1543–1558.

Yash Mantri is a PhD candidate in the Bioengineering department at UC San Diego. Previously he has worked on nanoparticle-based sensors for reactive oxygen and nitrogen species (RONS), explored the fundamentals behind nanoparticle-based photoacoustic signal generation, and undertaken human clinical studies to monitor wound healing using photoacoustic imaging.

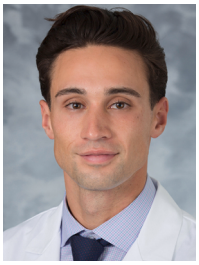

Tyler R. Dorobek is a M.D. Student (Class of 2025) at The University of Wisconsin School of Medicine and Public Health. After time in the U.S. Marine Corps, he attended UC San Diego attaining a B.S. in both Nanoengineering (Focus: Bioengineering) and Human Biology. His previous work at Sanford Consortium for Regenerative Medicine and UC San Diego School of Medicine Orthopedics focused in Regenerative Medicine, while other experiences include research in the Nanoengineering Department involving the intersection of biotechnology and nanoengineering.

Jason Tsujimoto is an undergraduate student in the Bioengineering department at UC San Diego. Previously, he has worked on ultrasound image analysis for use in wound sizing and photoacoustic image analysis for monitoring wound angiogenesis and healing. After earning his undergraduate degree, he plans to pursue a master's degree.

William F. Penny received his M.D. at Washington University in St. Louis, followed by an Internal Medicine Residency at UCLA and Fellowship in Cardiology and Interventional Cardiology at Beth Israel Hospital in Boston, MA. He is a Professor of Medicine at UC San Diego and the Director of the Cardiac Catheterization Laboratories at VA San Diego. He has extensive experience as a clinical trial investigator and a particular interest in studies involving devices and pharmacotherapies.

Pranav S. Garimella, MD, MPH is a nephrologist, epidemiologist, and Assistant Professor at UCSD in the Department of Medicine. His research funded by the NIH focuses on novel biomarkers for kidney and cardiovascular disease with a specific interest in peripheral artery disease in dialysis patients. He also serves as the Director of Acute Dialysis Services at UCSD Health.

Jesse V. Jokerst completed degrees in chemistry from Truman State University and UT Austin with postdoctoral training in Stanford Radiology. He is currently a Professor in the Department of Nanoengineering at UC San Diego where his lab uses imaging and nanotechnology to improve human health.